

Supplementary Material – MS 8179842

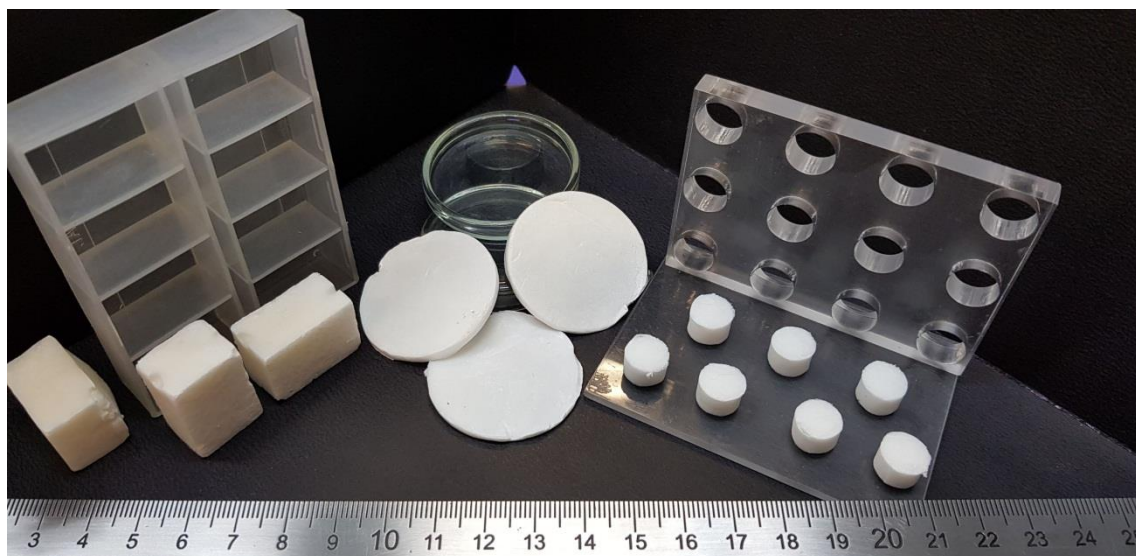


Figure SM1. Photographs of molds used and the resulting cryogels.

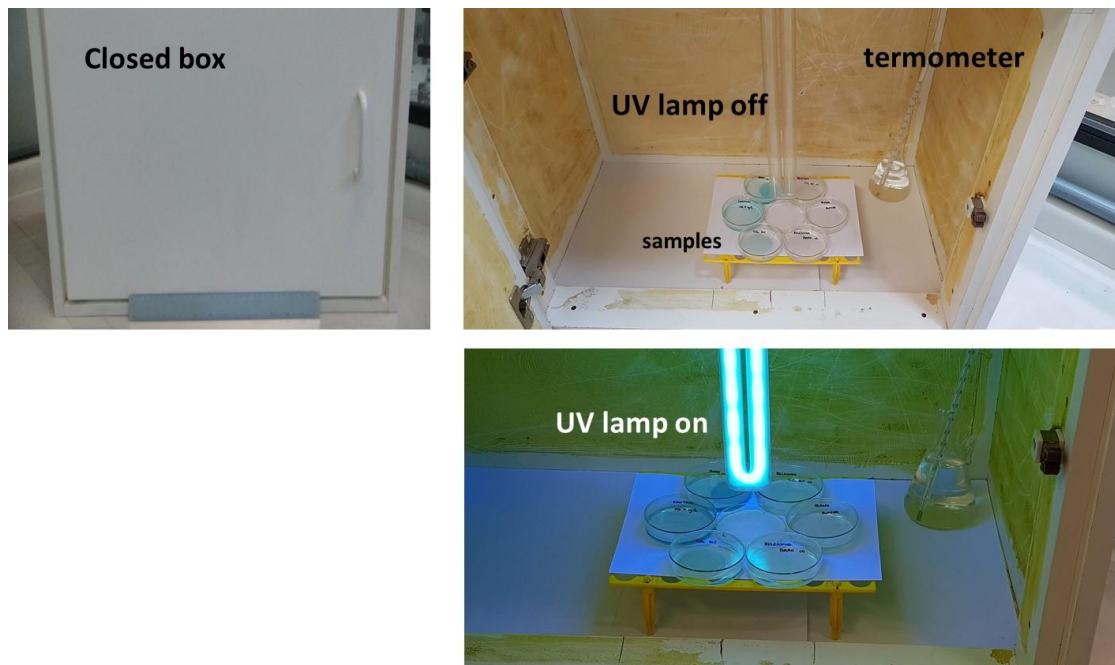


Figure SM2 – Experimental setup for the photocatalytic experiments.

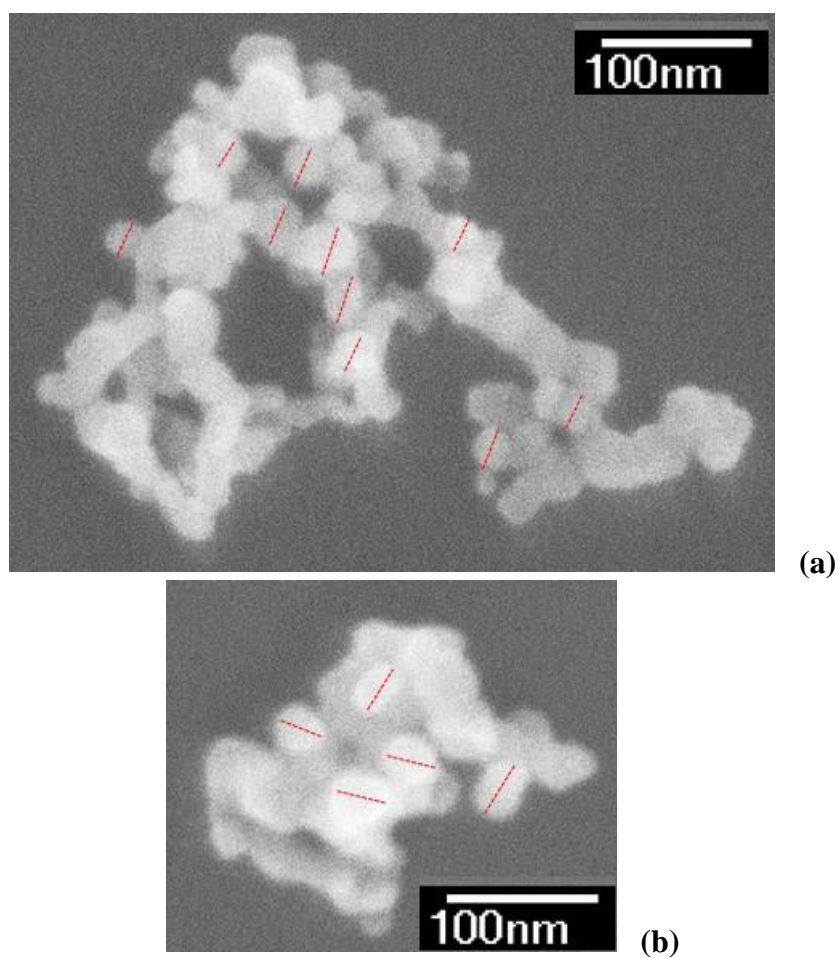


Figure SM3 – Typical SEM images of TiO₂ P25 particles. The particles were not coated with gold prior to the analyses because they are semiconductor. The mean size of TiO₂ particles amounted to (30 ± 5) nm, as an average of 15 measurements (red lines). The aggregates ranged from 100 nm to 500 nm, in agreement with the D_z values.

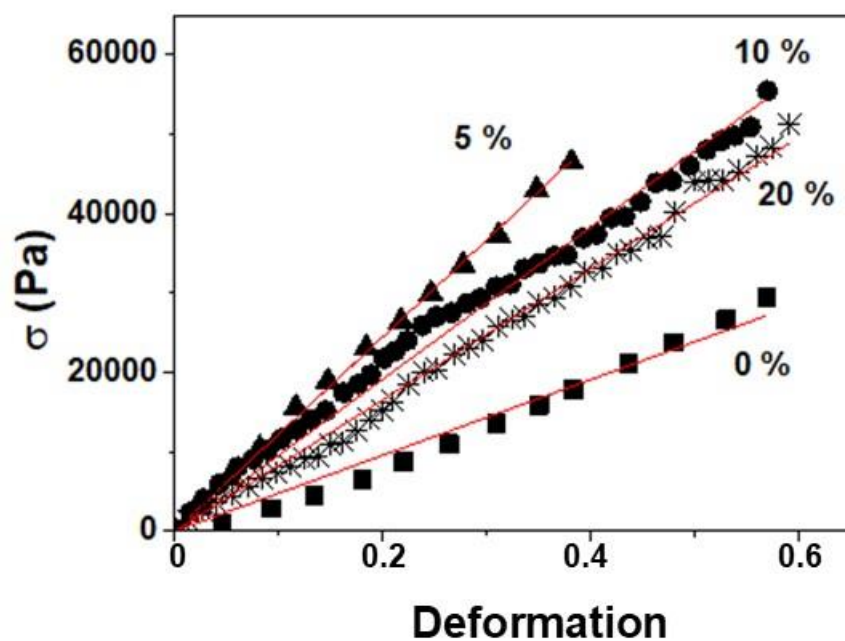


Figure SM4 – Typical compressive stress (σ)-strain curves determined for bare XG cryogels (0 %) and XG/TiO₂ cryogels with 5%, 10% and 20% TiO₂ prepared at pH 4.

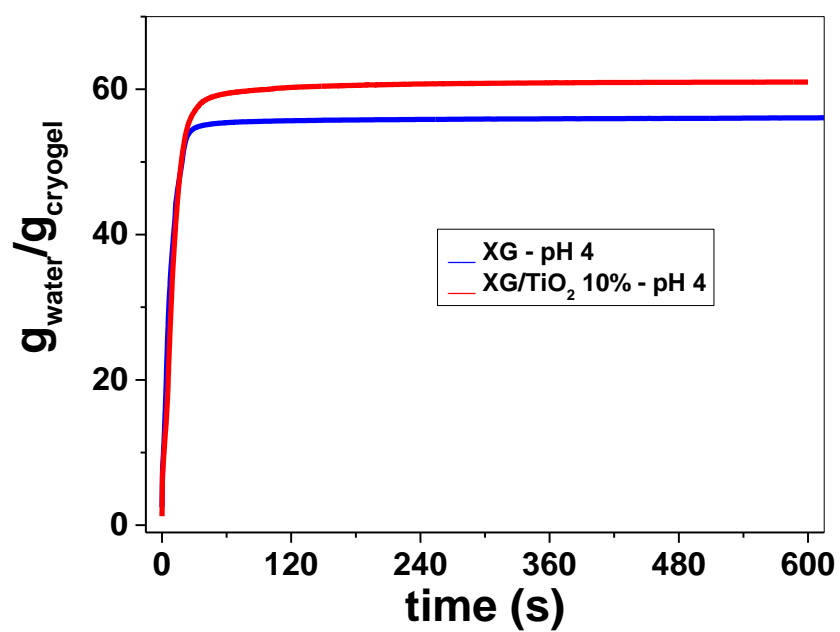


Figure SM5. Typical MilliQ water sorption curves determined for XG and XG/TiO₂ 10% cryogels prepared at pH 4, at (21 ± 1) °C.

Table SM1 – Bands assignment regarding the FTIR spectra obtained for XG and TiO₂ powder, and XG and XG/TiO₂ 10% cryogels.

Wavenumber (cm ⁻¹)	Band Assignment	Cryogel	Powder
3000-3500, broad	ν_{OH} intramolecular hydrogen bond	XG XG/TiO ₂ 10%	XG and TiO ₂
2910	$\nu_{as} CH_2$	XG XG/TiO ₂ 10%	XG
1725	$\nu C=O$ ester	XG XG/TiO ₂ 10%	-
1600	$\nu C=O$ carboxylic acid	XG XG/TiO ₂ 10%	XG
1515	δ C-H bending	XG/TiO ₂ 10%	-
1452	δ O-H carboxylic acid bending	XG/TiO ₂ 10%	-
1404	δ C-O-H carboxylic acid bending	XG	XG
1366	$\nu_{as} C=O$ carboxylate	XG XG/TiO ₂ 10%	XG
1195	C-O-H glycosidic ring	XG XG/TiO ₂ 10%	XG
1154	C-O-H glycosidic ring	XG XG/TiO ₂ 10%	XG

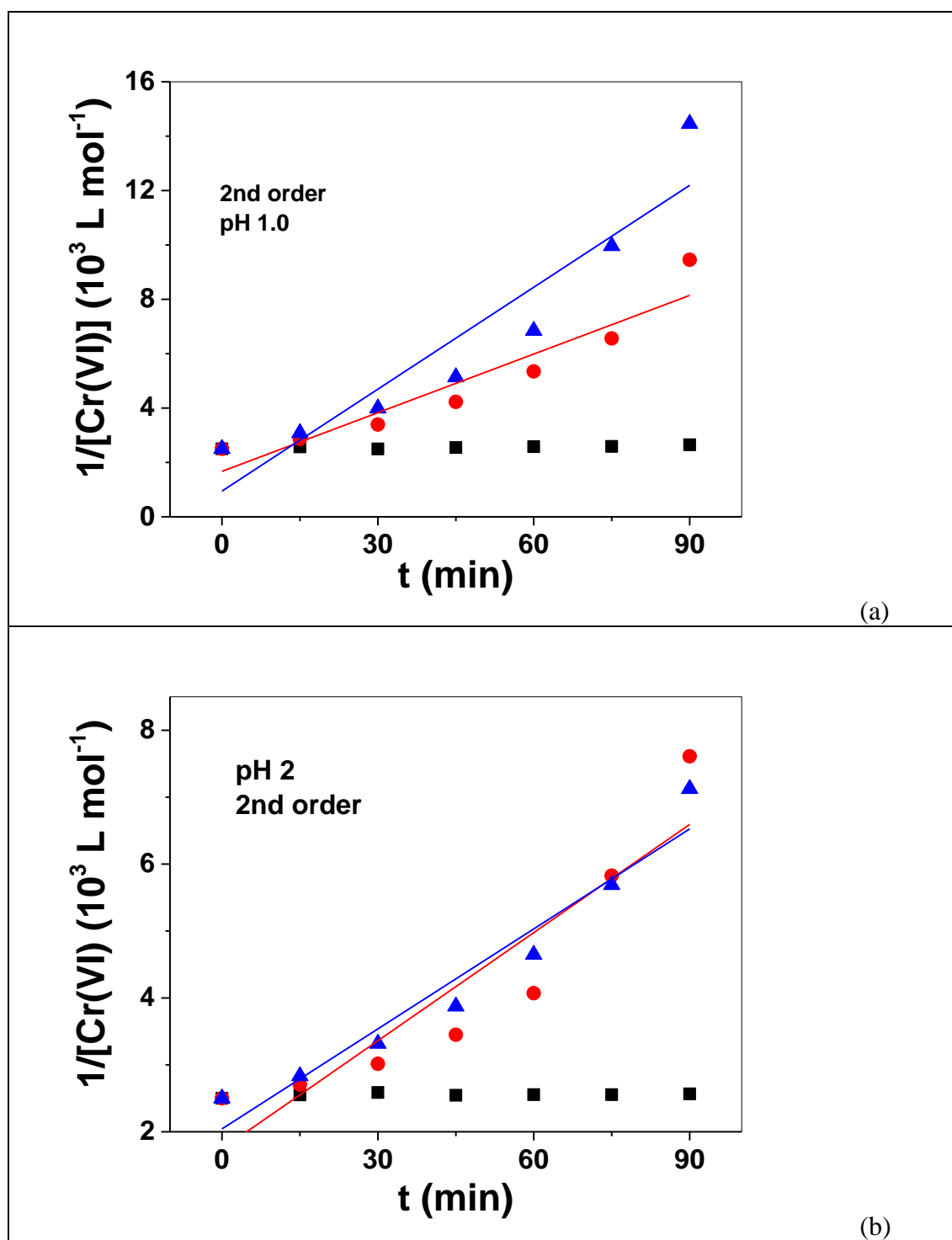


Figure SM 6. Fittings to second order kinetic model for the experimental data of reduction of Cr(VI) at (a) pH 1.0 and (b) pH 2.0 (see Figure 8).

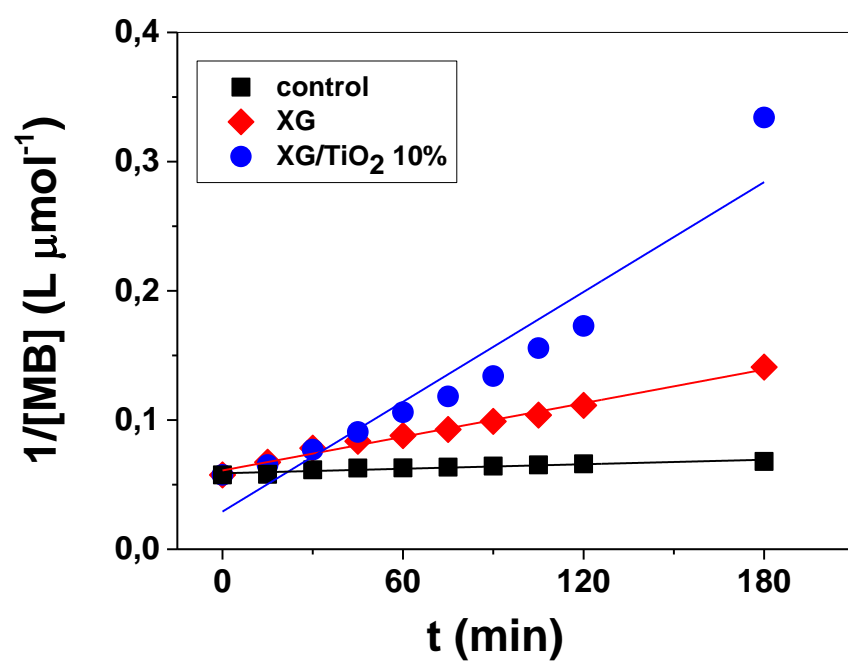


Figure SM 7. Fittings to second order kinetic model for the experimental data of degradation of MB at pH 7.0 (see Figure 9).